Interaction of the Tunnel Casing and the Newly Built Wing of the Railway Station Facility

Janusz P. Kogut[1*)], Elżbieta Pilecka[2)]

[1*)] Cracow University of Technology, ul. Warszawska 24, 31-155 Kraków, Poland, E-mail: jkogut@pk.edu.pl; ORCID 0000-0001-5728-1809
[2)] Cracow University of Technology, ul. Warszawska 24, 31-155 Kraków, Poland, E-mail: epilecka@pk.edu.pl; ORCID 0000-0002-1536-4291

https://doi.org/10.29227/IM-2025-02-02-042

Submission date: *2025-04-08* | Review date: *2025-05-09*

Abstract

Railway construction plays a vital role in the construction sector and is a key component of modern transportation infrastructure. In many countries, railways form the backbone of the transport system. Consequently, challenges that arise at the intersection of general construction and railway-specific engineering solutions are critical indicators of the overall quality of construction work. This paper focuses on analyzing the structural behavior observed during construction activities near a railway station building. These activities include the construction of a pedestrian tunnel leading to the railway platforms and the renovation of tracks adjacent to the building. The station's foundation lies in complex subsoil conditions. To address this, the design proposed the use of jet grouting columns, which serve both as structural support and as part of the tunnel casing. However, cracks were detected in the newly constructed wing of the station, raising concerns about project safety and potential delays. Following a review of the project documentation and a site inspection, the authors evaluated the execution methods for the facility's key components. The primary objective of this study is to determine the extent to which deviations from the original design may have influenced the behavior of the new station wing. A finite element method (FEM) model was developed based on geotechnical data. The simulation confirmed the effectiveness of the ground reinforcement and supported the original design assumptions regarding soil stabilization beneath the structure.

Keywords: *tunnel, excavations, jet-grouting, FEM*

1. Introduction

The subject of this paper is the analysis of the structural behaviour during construction works in the vicinity of the station building, i.e. the construction of the tunnel for the passage to the railway platforms and the renovation of the railway track directly adjacent to the building. The aim of the study is to answer the question to what extent the contractor's deviation from the design study may affect the behaviour of the newly built wing of the railway station building. The basis of the work is the analysis of materials constituting the construction design and the analysis of the serviceability limit state in relation to the foundation slab of the newly built wing and the substrate identified on the basis of the on-site inspection, as well as tests performed during the tunnel works [9]. The numerical simulations are carried out using the finite element method (FEM) and the Midas program. The modernised railway line is one of the most important investments currently implemented by local railways. It is part of the project of building the international railway line Rail Baltica, which will connect Western Europe with the Baltic States and Finland. The effect of the investment will be more convenient and faster travel on the route east of Warsaw. Once all work on the line is completed, rail travel is expected to improve significantly and the line's capacity will also increase, allowing for more trains to be serviced. During the investment, the railway station was renovated. Additionally, a new wing of the station was built, along with a designed and constructed access tunnel to the platforms. In order to strengthen the ground under the existing station building, the designer proposed jet-grouting technology to secure the facility.

Jet-grouting, or high-pressure jet injection aimed at improving the bearing capacity of the soil, is widely used in civil engineering and it is applied in almost all types of soil. It involves the destruction of the natural structure of the substrate by means of a grout introduced at a pressure of 30–50 MPa with a flow rate of 50–450 l/min [14]. It is mixing and partially replacing the existing substrate with a binding agent. In this way, injection elements (columns, walls, slabs, blocks) are formed from concreting soil, the compressive strength of which, depending on the type of soil medium, can be from about 1 MPa in organic soils, of about 5 MPa in clays, and about 15-20 MPa in the case of forming columns in sands and gravels, which is quite sufficient when making deep foundations. During the works, the spoil is extracted, i.e. excess of the grout-soil mixture, flowing to the surface through the space between the rod and the wall of the injection hole, the excess of which is removed. High-pressure jet-grouting technology is used both for strengthening the ground and for forming screens that limit the inflow of water. Strengthening, i.e. soil cementation, most often concerns the foundation of buildings adjacent to a deep excavation, or the reconstruction and repair of existing buildings. Unfortunately, sometimes this technology may be performed incorrectly, especially at the stage of connecting with the foundations when performing this work. Additionally, the diameters of the columns may significantly differ from the actual dimensions [11-13].

Depending on the amount of materials used and the method of their application, three injection systems are distinguished: single, double – water and air – and triple. The most commonly used single system is based on the use of a stream of one liquid, usually cement grout. In the case of a double system, the injection of the grout (usually cement grout) is supported by another medium: compressed (usually air – the so-called double air system) or water (double water system), supporting the loosening of the soil. There is also a triple injection system, which assumes that the destruction of the soil structure is achieved by a high-energy water stream supported by compressed air, while the cementation of the soil occurs as a result of the application of the grout stream. The injection system used affects the unit cement consumption and the time needed to form columns and the cement-soil parameters (including strength) and the diameters of the obtained elements. In addition to the type of injection system, other factors also affect the possible column diameters, such as: the type and condition of the soil,

the shape and location of the injection nozzles, the design of the injection monitor and the technological parameters of the injection, i.e. injection pressure, the number and diameter of injection nozzles, the speed of pulling the injection rod, the rotational speed of the injection rod or the density of the grout and, in the case of double and triple systems, the flow and pressure of air and/or water. Typical dimensions of the diameters of the formed elements are from 0.4 m upwards. Already at the design stage, many factors determining the diameters of the columns should be taken into account and it should be remembered that the expected diameter of the injection elements should be verified after the work has been completed. Therefore, it is considered good practice to dig out the upper parts of the finished columns and hack off their heads. During the work, a site visit took place at the construction site of the railway station. Representatives of the contractor together with the authors of this article inspected the exposed fragment of the heads of the jet-grouting columns. These columns were located directly under the foundation slab of the newly built wing of the station. Figure 1 shows the visible palisade directly under the station building, additionally propped before the concreting began.

Fig. 1. Palisade constructed under the visible foundation slab of the railway station building

Figure 2 shows the exposed tops of jet-grouting columns located directly under the station building. Jet-grouting columns are visible approximately 1.50 m below ground level. Their heads have narrowed significantly and only the native soil remains directly under the foundation slab. This situation causes the structure to behave in a horizontal direction from earth pressure forces and exposes the structure founded on the slab to additional settlements. The designer anticipated such behaviour in the short period between the tunnel excavation and concreting of the tunnel casing. In the executive design, the palisade was supplemented with ground anchors (approximately 9 m long), the heads of which were designed deep below the palisade. As a result, the pressure forces were to be balanced by additional tensile forces transferred by the ground anchors. Figure 3 shows the real “anchoring”, where instead of ground anchors, some kind of nailing is implemented, and the loosely hanging anchoring shows that it is completely ineffective. In fact, it is located in the native soil, which results finally in the lack of transfer of tensile forces and does not balance the earth pressure at all.

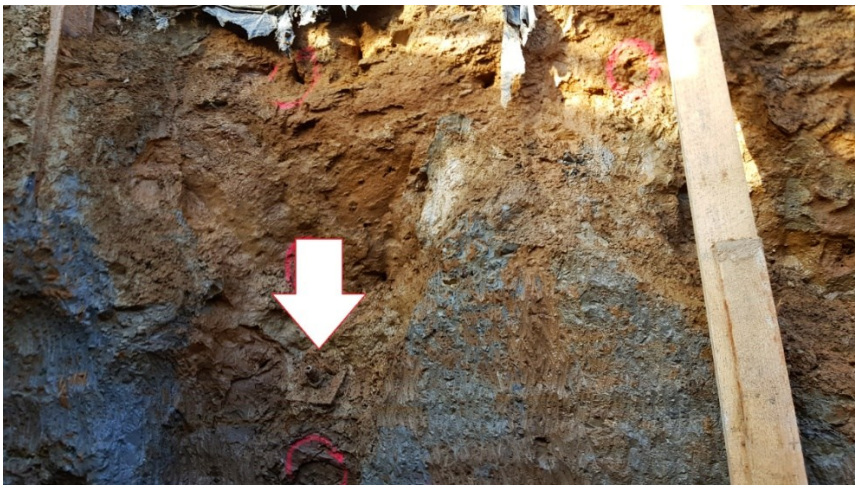

Fig. 2. A palisade made of jet-grouting with a visible ground nail with a loosely suspended anchor plate located in the native soil

Due to the quality of the works and especially the regular occurrence of a high groundwater table, the designer recommended the construction of four rows of jet-grouting columns. In this way, they cut off the flow of water towards the tunnel casing and ensured tightness due to the low water permeability coefficient of the clay. Figure 3 shows the solution proposed by the designer, taking into account both the protection to the earth pressure and the water flow reduction. The four rows of jet-grouting columns that interpenetrate each other and create a rocky whole ensure tightness and continuity along the tunnel walls. Additionally, they provide strong support for the foundation slab.

To assess the integrity of the jet-grouting barrier, a method was proposed to verify whether the palisade of jet-grouting columns is continuous and impermeable. Figure 4 illustrates the proposed borehole, drilled at an oblique angle of approximately 30 degrees from the horizontal plane. The core sample obtained through this method should confirm whether the column barrier has been constructed in accordance with the designer’s specifications. Figure 5 presents the actual borehole carried out following the arrangements made during the

on-site inspection. The results indicate that the works were not executed as per the design— the entire borehole consists of soil material, with no evidence of the expected hardened grout. This suggests that the jet-grouting columns, as designed, are absent at this location.

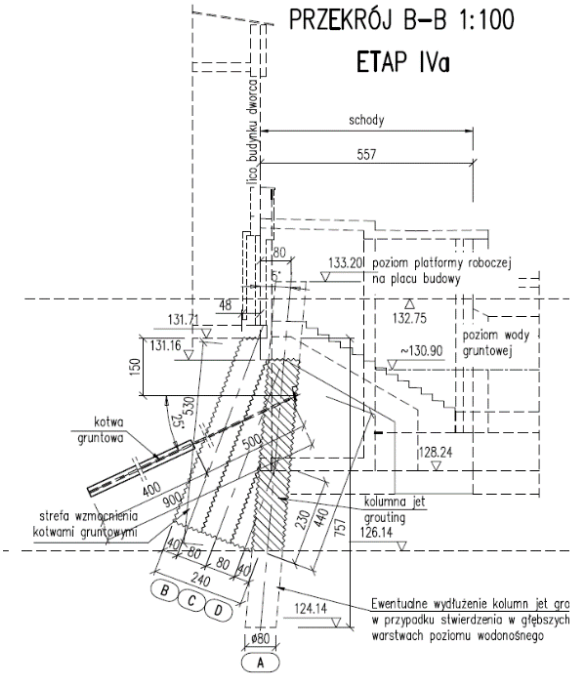

Fig. 3. Design solution including the construction of 4 rows of columns and a ground anchor

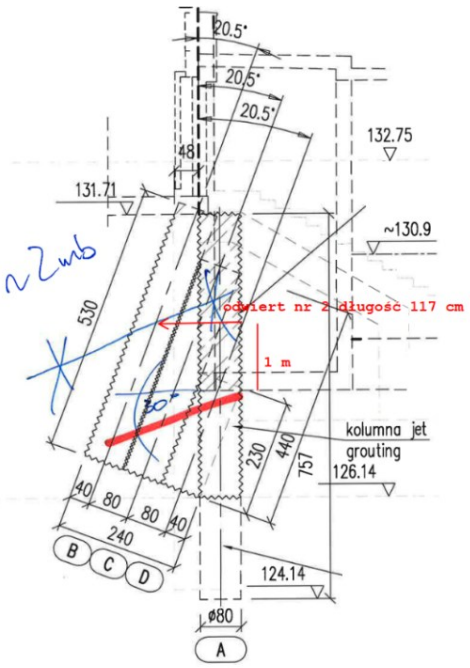

Fig. 4. The method proposed during the on-site inspection to check whether the palisade is continuous and tight.

Fig. 5. A drill core examination revealed that the jet grouting barrier is discontinuous and permeable, with visible inclusions of soil material..

2. Groundwater

Groundwater can affect the quality of foundations and the subsoil. If groundwater is contaminated, it can negatively affect the quality of concrete and cause its qualitative weakening or increase, e.g. its shrinkage. However, groundwater can affect the process of concrete maturation, which can result in its inhomogeneity and different mechanical properties. Additionally, groundwater can affect the process of concrete hardening, which may lead to the formation of air bubbles in the concrete or its scratching or cracking. Therefore, when designing and constructing foundations of structures, water and geological conditions should be taken into account and the technology of concrete production and application should be selected consequently. Contaminants in groundwater, such as mineral salts or organic compounds, may penetrate the concrete and affect its physical and chemical properties, such as compressive strength, modulus of elasticity or resistance to frost and salt. Additionally, contaminants can affect the cement hydration process, leading to the formation of fewer hydrates and a reduction in their durability, resulting in lower concrete strength.

Water or soil contamination may prevent construction work in various situations, for example when [8-9]:

- groundwater is too high - if the groundwater level is too high in relation to the excavation level, it may be necessary to carry out drainage or dewatering work before and/or during construction work.
- groundwater is contaminated - if the groundwater contains contaminants, this can affect the quality of concrete or other building materials and lead to improper functioning of the building's foundations. In such cases, it may be necessary to clean the ground or use other technical solutions.
- ground is contaminated - if the ground is contaminated with toxic substances, construction work may be impossible or require special precautions.

Such situations occur when foundations are located on industrial sites or when there are uncontrolled embankments in the ground, in which water can flow freely and additionally enter into the tunnels and excavations. It may also locally cause an increase in pore water pressure and contribute to the weakening of the physical properties of native soils, e.g. through suffusion process.

3. Analysis of the design solution

Bearing in mind these facts, it has been proposed to check the behaviour of the subsoil under the railway station building by analysing a number of cases related to the actual and planned phase. In both cases, the behavior of the subsoil with a low (ZWG 1) and high (ZWG 2) groundwater table is taken into account. The numerical calculations took into account the staging of the works and the execution of the

excavation in the vicinity of the building. The numerical calculations using the finite element method (FEM) in the Midas program has been performed as follows. In the first step, the excavation and construction of the foundation slab, then the loading of forces representing the permanent and variable load of the newly constructed station building are taken into account. In the next step, the construction of jet-grouting columns is checked in two variants: the designer and alternate - identified after the site visit. Then, the execution of the excavation of the planned tunnel under the platforms was taken into account. The parameters for the calculations are obtained from the documentation, and later they are verified by testing samples collected during the site visit. The soil material has been analysed in the laboratory of the Department of Geotechnics and Strength of Materials of the Cracow University of Technology in order to determine the native subsoil.

For the variants described above, numerical models describing the analysed situations in a plane strain state have been built. The Midas GTX program used by the Department of Geotechnics and Strength of Materials is utilized. The calculations are made in stages, assuming the Coulomb-Mohr stress model and mapping the serviceability limit states [1-2, 10]. The total values of the angle of internal friction φ(n) = 14 degrees and the cohesion c(n) = 15 kPa is assumed. In the second case, the effective values of the angle of internal friction equal to φ' = 20 degrees and the effective cohesion equal to c' = 11 kPa is assumed.

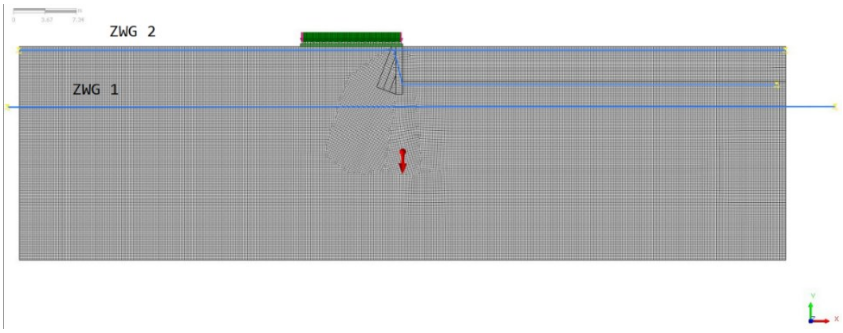

Fig. 6. FEM mesh used to calculate the initial state of the subgrade loaded with a structure placed on a slab and the dead weight of the ground. Two levels of groundwater visible

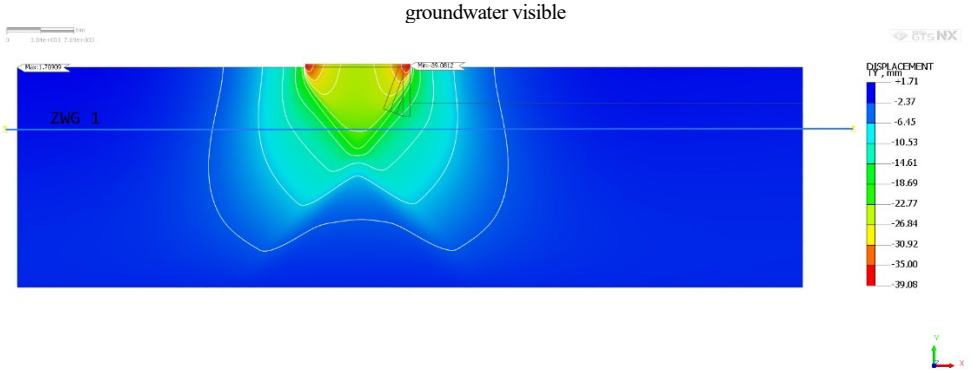

Fig. 7. Image of vertical displacements at the initial state and the lower level of the groundwater table (ZWG 1) for the values of total parameters

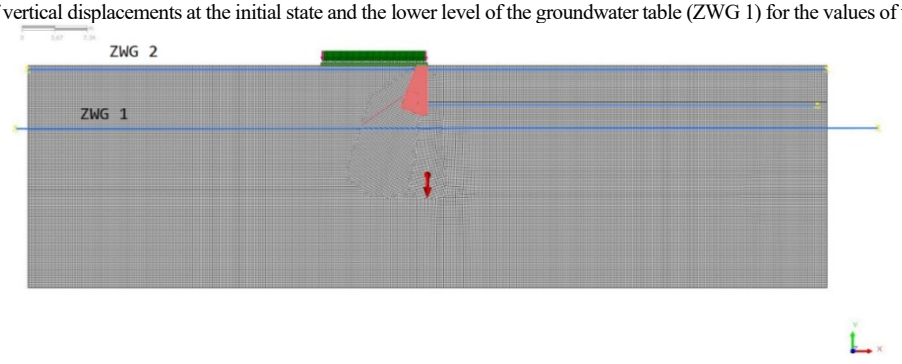

Fig. 8. FEM mesh used to calculate the design state of the subgrade loaded with a structure placed on a slab and the dead weight of the ground after the jet-grouting columns and anchors were installed. Two levels of groundwater visible

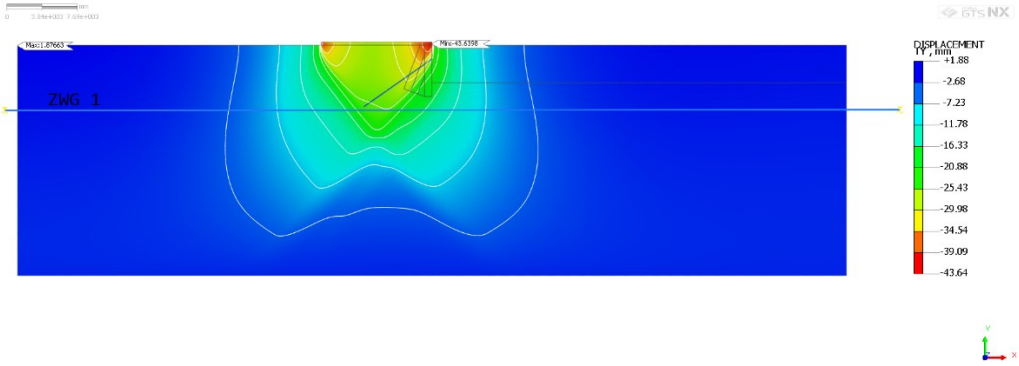

Fig. 9. Image of vertical displacements at the design state and the lower level of the groundwater table after the jet-grouting columns and anchors were installed for the values of total parameters

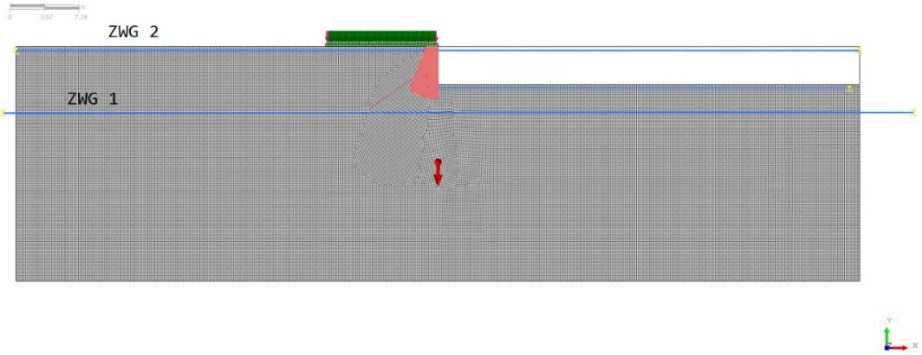

Fig. 10. FEM mesh used to calculate the design state of the subgrade loaded with a structure placed on a slab and the dead weight of the ground after the tunnel excavation. Two levels of groundwater visible

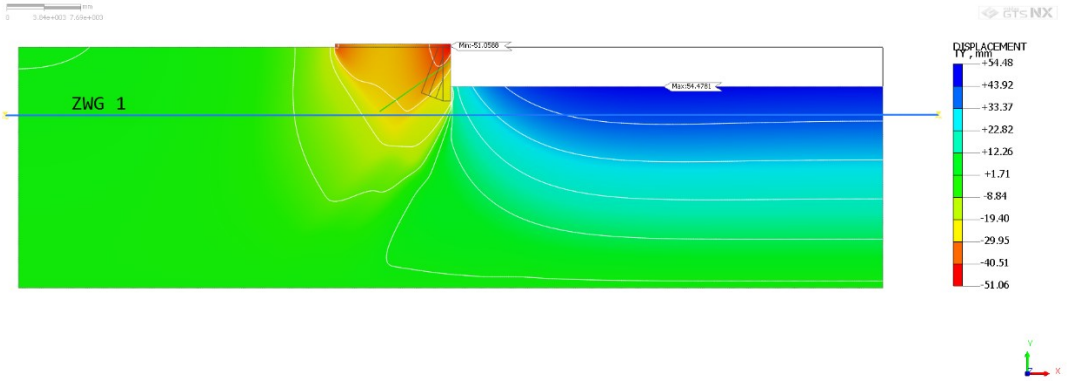

Fig. 11. Image of vertical displacements at the design state and the lower level of the groundwater table after the tunnel excavation for the values of total parameters

Figure 6 presents the FEM mesh used to calculate the initial state of the ground loaded with a building placed on a slab and the soil's self weight. Two levels of groundwater are visible in the figure. The low water and the high water level and water flow in relation to the tight wall made of jet-grouting columns. Figure 7 shows the image of vertical displacements at the initial state and the low water level. Figure 8 presents the FEM mesh used to calculate the design condition of the subsoil loaded with a structure placed on a slab and the self-weight of the soil after the installation of jet-grouting columns and anchors. For the mesh adopted in this way, vertical displacements have been calculated at the design condition and the low water table, which are visible in Figure 9. Figure 10 shows the FEM mesh used to calculate the design condition of the subsoil loaded with the structure placed on the slab and the self-weight of the soil after the tunnel has been excavated. Figure 11 shows the image of vertical displacements at the design state and the low water table after the tunnel excavation. Based on the calculations of the situation from Figures 7-11, a summary of vertical displacements (settlement) of the corner of the foundation slab in the B-B cross-section for the design state is visible in Table 1, taking into account the low water table. All calculations refer to the total soil parameters.

Then, similar calculations are performed taking into account the effective parameters of the subsoil. The same FEM meshes are used. Figure 12 presents the image of vertical displacements at the initial state and the low water table. Figure 13 shows the image of vertical displacements at the design state and the low water table after the jet-grouting columns and anchors have been completed. Figure 14 presents the image of vertical displacements at the design state after the tunnel excavation for the values of effective parameters. The results from Figures 12-14 were also included in the summary prepared for the above-mentioned calculation states in Table 1.

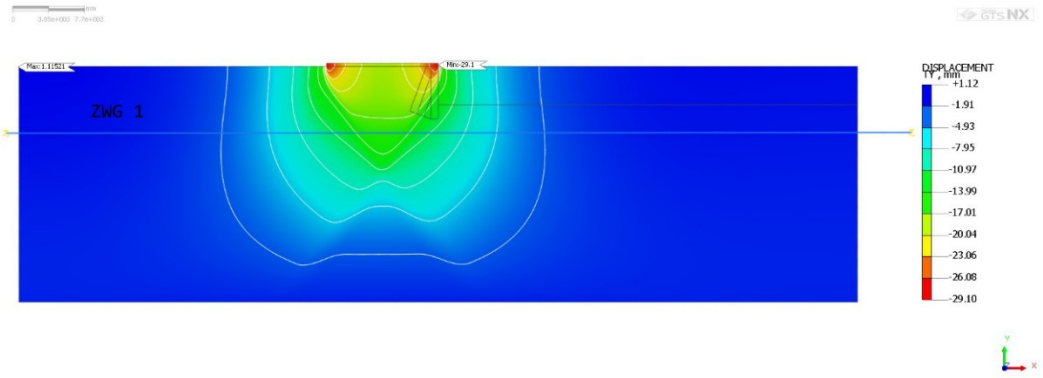

Fig. 12. Image of vertical displacements at the initial state and the lower level of the groundwater table, taking into account the effective parameters of the subsoil

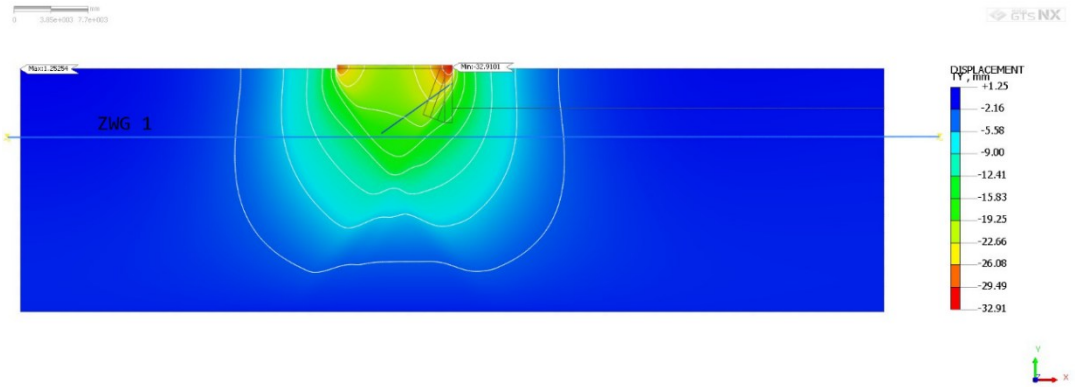

Fig. 13. Image of vertical displacements at the design state and the lower level of the groundwater table after the construction of jet-grouting columns and anchors and taking into account the effective parameters of the subsoil

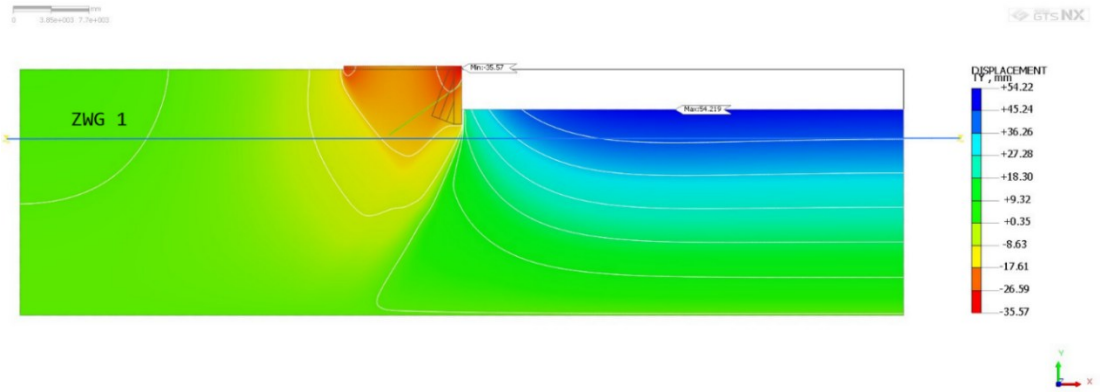

Fig. 14. Image of vertical displacements at the design state and the lower level of the groundwater table after the tunnel excavation, calculated for the values of effective parameters

Tab. 1. Vertical displacements of the slab corner in the design state, taking into account the low water level

Parameters	Vertical displacements [mm]			
	after consolidation	with jet-grouting columns	with tunnel excavation	Final
total	39,1	43,6	51,1	7,5
effective	29,1	32,9	35,6	2,7

Figure 15 shows the image of vertical displacements at the initial state and the highest water table. For the mesh adopted in Figure 8, vertical displacements are calculated at the design condition which are visible in Figure 16. The FEM mesh from Figure 10 is used to calculate the design condition of the subsoil loaded with the structure placed on the slab and the self-weight of the soil after the tunnel has been excavated. Figure 17 shows the image of vertical displacements at the design state and the highest water table after the tunnel excavation. Based on the calculations of the situations from Figures 15-17, a summary of vertical displacements (settlement) of the corner of the foundation slab in the B-B cross-section is prepared in Table 2 for the design state, taking into account the highest water table. All calculations refer to the total soil parameters.

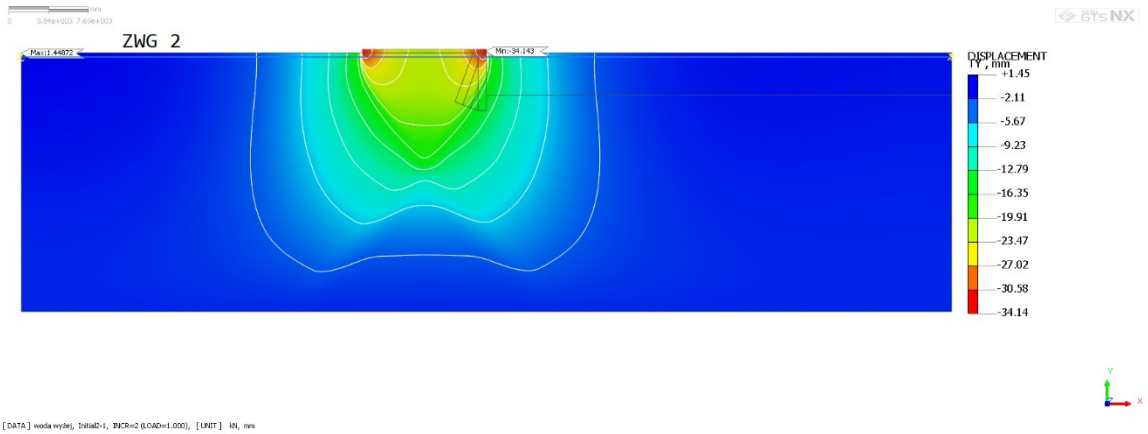

Fig. 15. Image of vertical displacements at the initial state and the upper level of the groundwater table (ZWG 2) for the values of total parameters

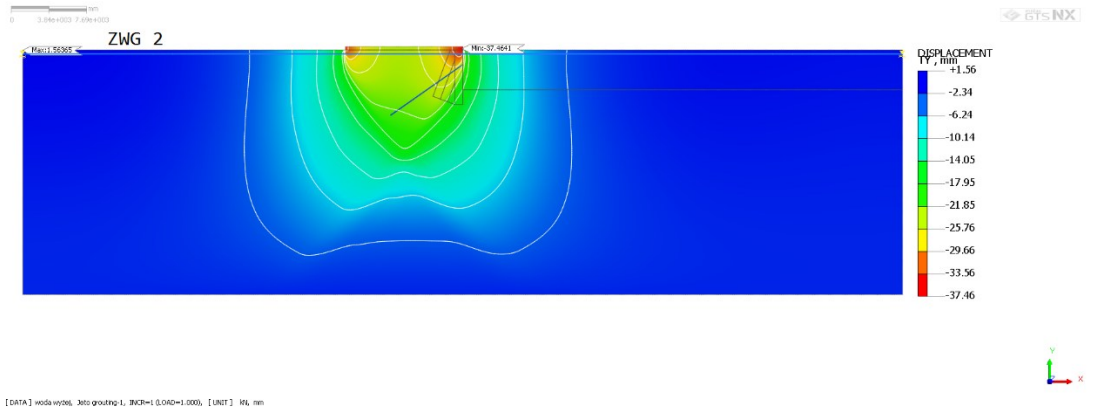

Fig. 16. Image of vertical displacements at the design state and the upper level of the groundwater table after the completion of jet-grouting columns and anchors for the values of total parameters

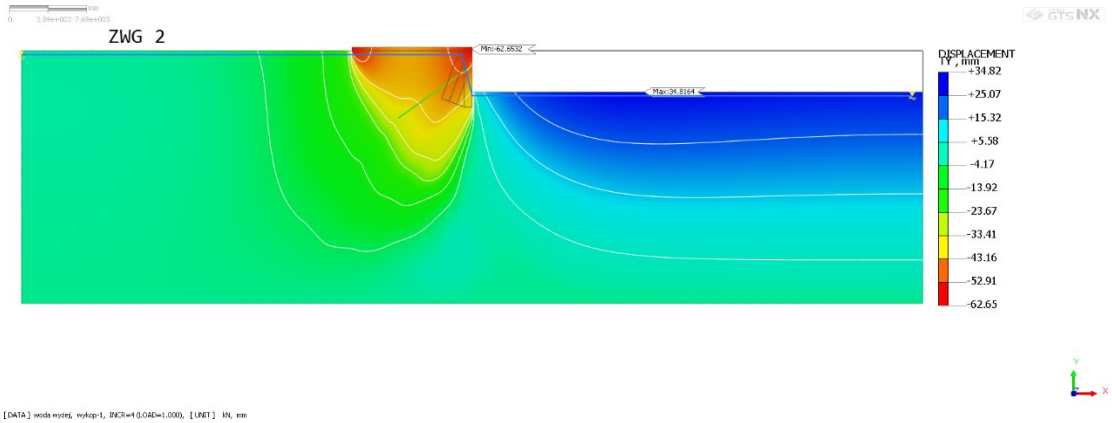

Fig. 17. Image of vertical displacements at the design state and the upper level of the groundwater table after the completion of the tunnel excavation for the values of total parameters

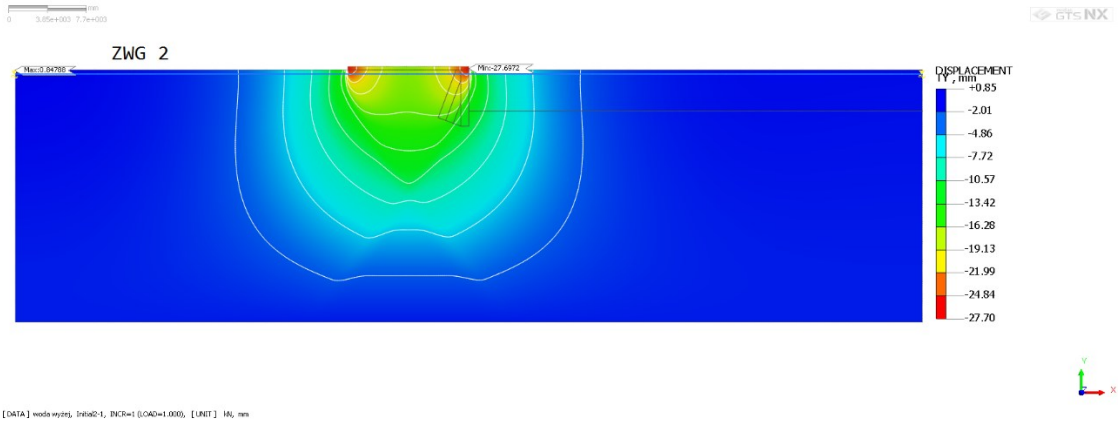

Fig. 18. Image of vertical displacements at the initial state and the upper level of the groundwater table for the values of effective parameters

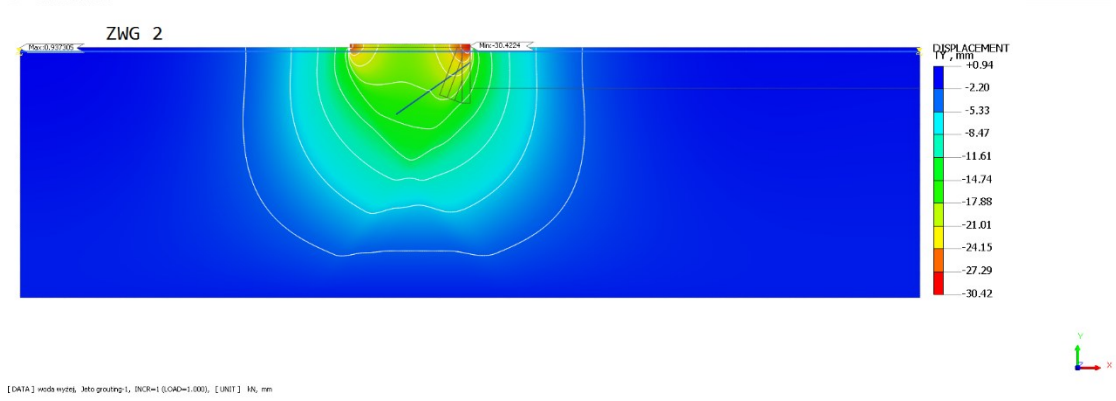

Fig. 19. Image of vertical displacements at the design state and the upper level of the groundwater table after the completion of the jet-grouting columns and anchors for the values of effective parameters

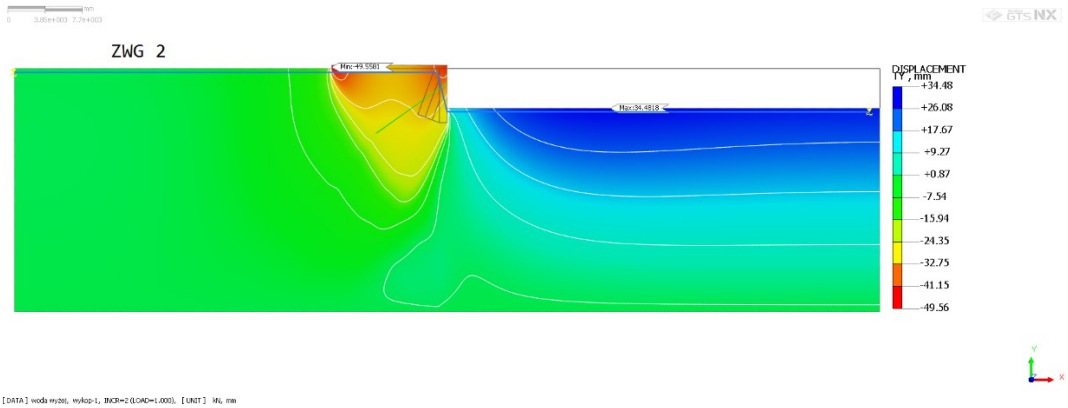

Fig. 20. Image of vertical displacements at the design state and the upper level of the groundwater table after the completion of the tunnel excavation for the values of effective parameters

Tab. 2. Vertical displacements of the slab corner in the design state, taking into account the high water level

Parameters	Vertical displacements [mm]			
	after consolidation	with jet-grouting columns	with tunnel excavation	Final
total	34,1	37,5	62,6	25,1
effective	27,7	30,4	46,0	15,6

Then, similar calculation situations have been analysed taking into account the effective parameters of the subsoil. The same FEM meshes are used. Figure 18 presents the image of vertical displacements at the initial state and the highest water table. Figure 19 shows the image of vertical displacements at the design state after the jet-grouting columns and anchors have been completed. Figure 20 presents the image of vertical displacements at the design state after the tunnel excavation. The results from Figures 18-20 are included in the comparison prepared for the above calculation stages in Table 2.

4. Analysis of the implementation solution for underpinning the foundation slab from the track side

Here, the implementation of solution for the foundation slab underpinning the newly constructed wing of the railway station building is analysed. Similarly to the previous chapter, the behaviour of the foundation slab loaded as in the case of the design solution is analysed, taking into account both the total and the effective parameters of the ground. The calculations are carried out for both the low and the highest groundwater table. The FEM meshes adopted for calculations for the individual stages of analysis are still presented, as they differ from those for which the design state calculations have been carried out. The differences result from the assumption of actually made jet-grouting piles and the lack of effective anchoring.

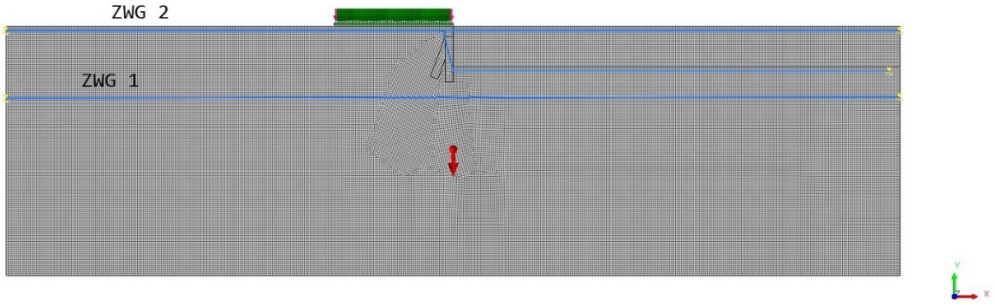

Fig. 21. FEM mesh used to calculate the initial state of the ground loaded with a structure placed on a slab and the soil's own weight. Two levels of groundwater visible

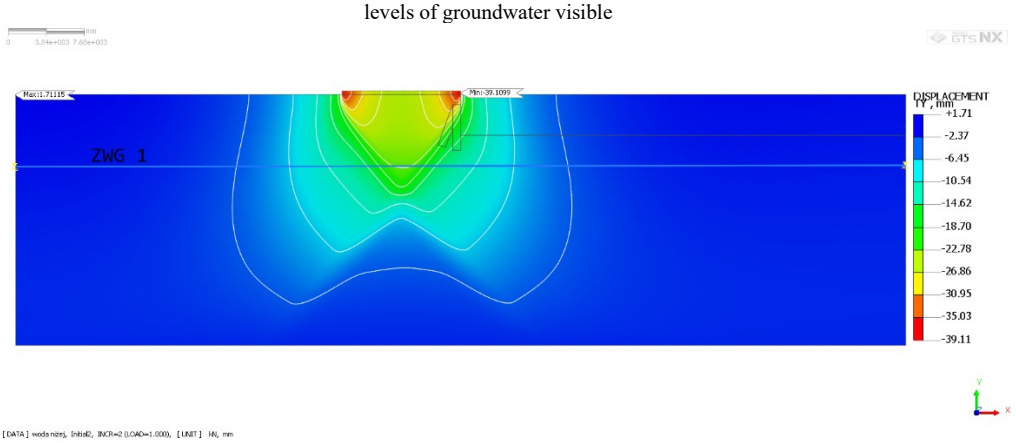

Fig. 22. Image of vertical displacements at the initial state and the lower level of the groundwater table for the values of total parameters

Fig. 23. FEM mesh used to calculate the final state of the subgrade loaded with a structure placed on a slab and the dead weight of the ground after the construction of jet-grouting columns without anchors. Two levels of groundwater visible

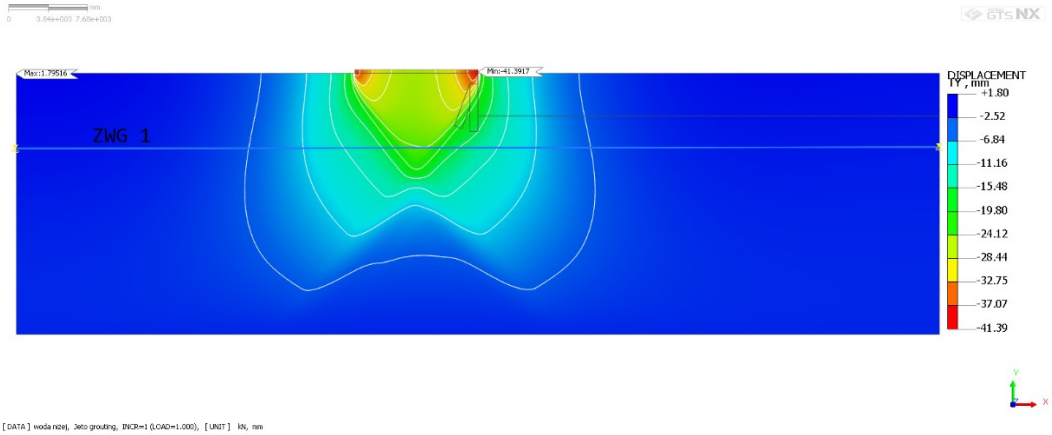

Fig. 24. Image of vertical displacements at the existing state and the lower level of the groundwater table after the construction of jet-grouting columns and without anchors for the values of total parameters

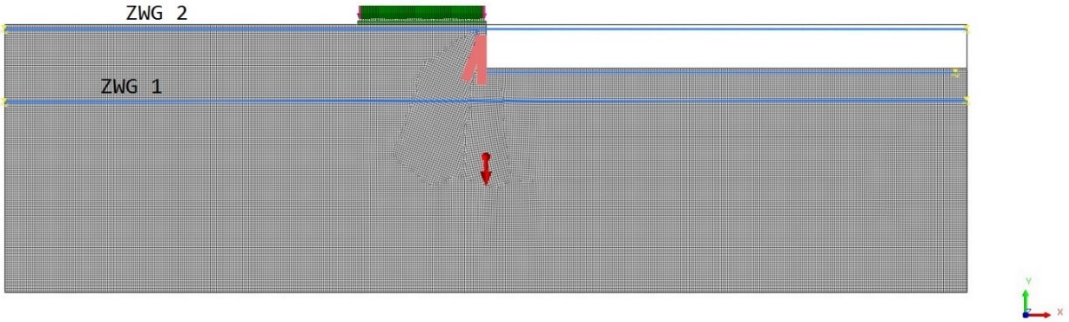

Fig. 25. FEM mesh used to calculate the existing state of the subgrade loaded with a structure placed on a slab and the dead weight of the ground after the tunnel excavation. Two levels of groundwater visible

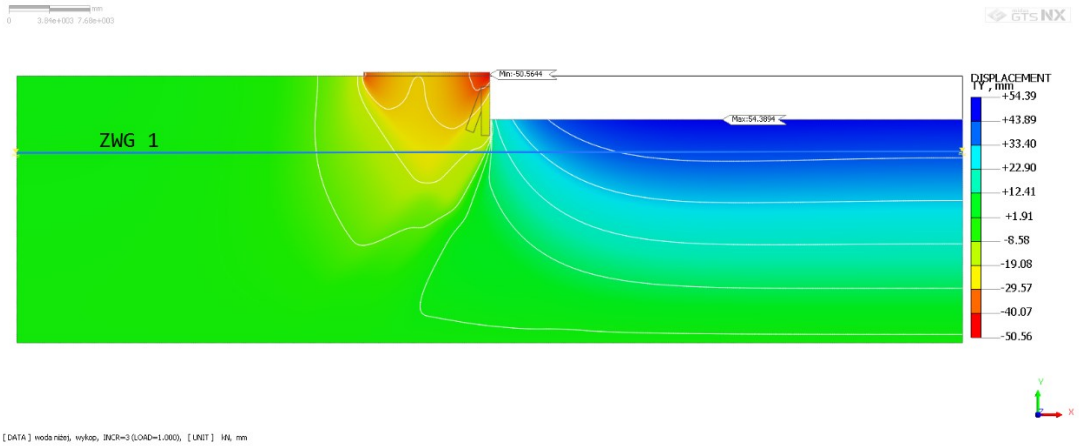

Fig. 26. Image of vertical displacements at the existing state and the lower level of the groundwater table after the tunnel excavation for the values of total parameters

Figure 21 shows the FEM mesh used to calculate the initial state of the subgrade loaded with a structure placed on a slab and the dead weight of the soil. Two levels of groundwater are visible in the figure. The low water level and the highest water level and water flow in relation to the wall made of jet-grouting columns. Figure 22 shows the image of vertical displacements at the initial state and the lower level of the groundwater table. Figure 23 shows the FEM mesh applied to calculate the existing state of the subgrade loaded

with a structure placed on a slab and the dead weight of the soil after the jet-grouting columns have been made without taking into account the anchors. For the mesh adopted in this way, vertical displacements are calculated at the existing condition and the lower groundwater table, which are visible in Figure 24. Figure 25 shows the FEM mesh used to calculate the condition of the existing subsoil loaded with the structure placed on the slab and the self-weight of the soil after the tunnel has been excavated. Figure 26 shows the image of the vertical displacements for the existing condition and the low groundwater table after the tunnel excavation. Based on the calculations of the situations from Figures 21-36, a summary of the vertical displacements (the settlements) of the corner of the foundation slab in the B-B cross-section is arranged in Table 3 for the existing condition, taking into account the low water level. All calculations refer to the condition in which the calculations are made for the values of the total soil parameters.

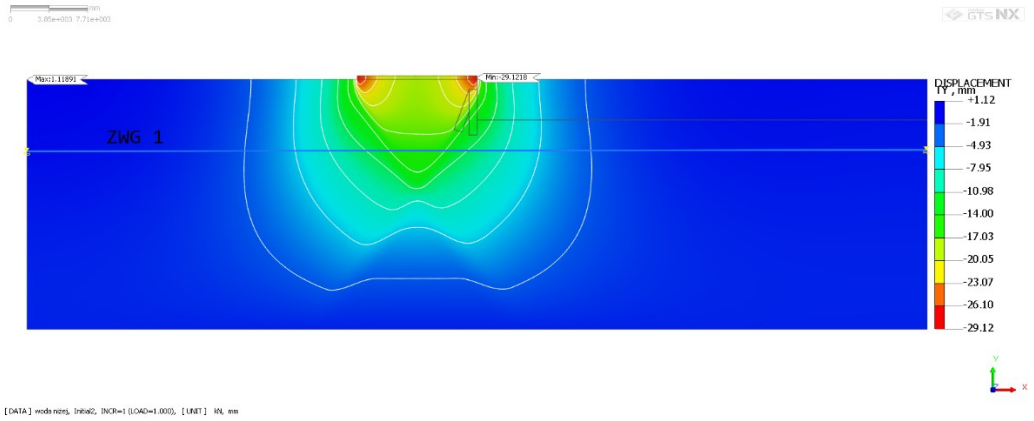

Fig. 27. Image of vertical displacements at the initial state and the lower level of the groundwater table, taking into account the effective parameters of the subsoil

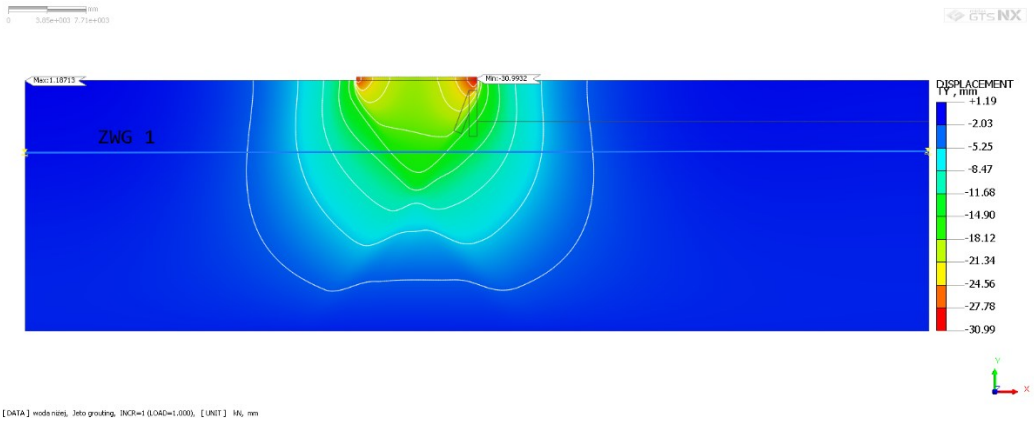

Fig. 28. Image of vertical displacements at the existing state and the lower level of the groundwater table after the construction of jet-grouting columns and anchors and taking into account the effective parameters of the subsoil

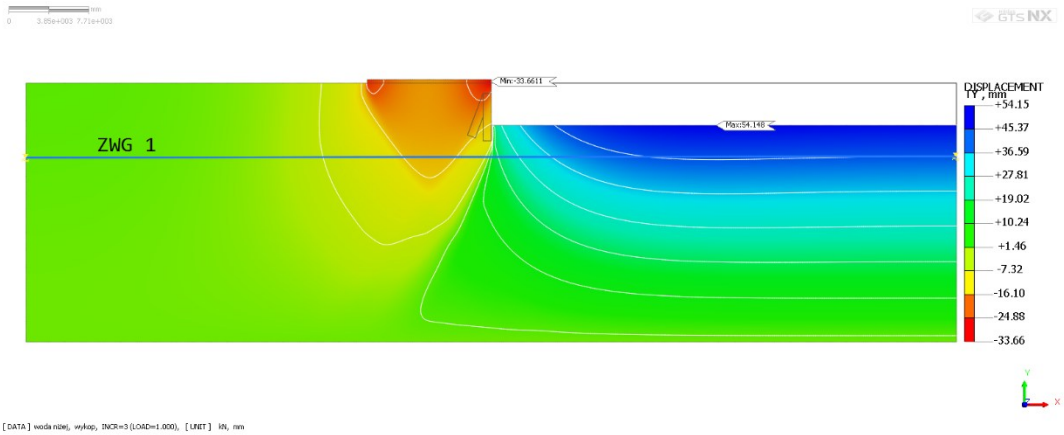

Fig. 29. Image of vertical displacements at the existing state and the lower level of the groundwater table after the tunnel excavation, calculated for the values of effective parameters

Then, similarly to Chapter 3, the calculation situations are analysed taking into account the effective parameters of the subsoil. The same FEM meshes from Figures 21, 23 and 25 were used. Figure 27 presents the image of vertical displacements at the initial state and the low water level. Figure 28 shows the image of vertical displacements at the existing state after the construction of jet-grouting columns and without anchors. Figure 29 presents the image of vertical displacements at the existing state after the tunnel excavation. The results from Figures 27-29 are also included in the comparison prepared for the above-mentioned calculation states in Table 3.

Tab. 3. Vertical displacements of the slab corner in the actual state, taking into account the low water table

Parameters	Vertical displacements [mm]			
	after consolidation	with jet-grouting columns	with tunnel excavation	Final
total	39,1	41,4	50,6	9,2
effective	29,1	31,0	33,7	2,7

Figure 30 shows the image of vertical displacements at the initial state and the highest groundwater table. For the mesh adopted from Figure 21, vertical displacements are calculated at the existing state and the upper level of the groundwater table, which are visible in Figure 31. The FEM mesh from Figure 25 is utilized to calculate the existing state of the subgrade loaded with the structure founded on the slab and the dead weight of the soil after the tunnel excavation. Figure 32 shows the image of vertical displacements at the existing state after the tunnel excavation. Based on the calculations of the situations from Figures 30-32, a summary of vertical displacements (the settlements) of the corner of the foundation slab in the B-B cross-section is prepared in Table 4 for the existing state, taking into account the highest groundwater table. All calculations refer to the total soil parameters.

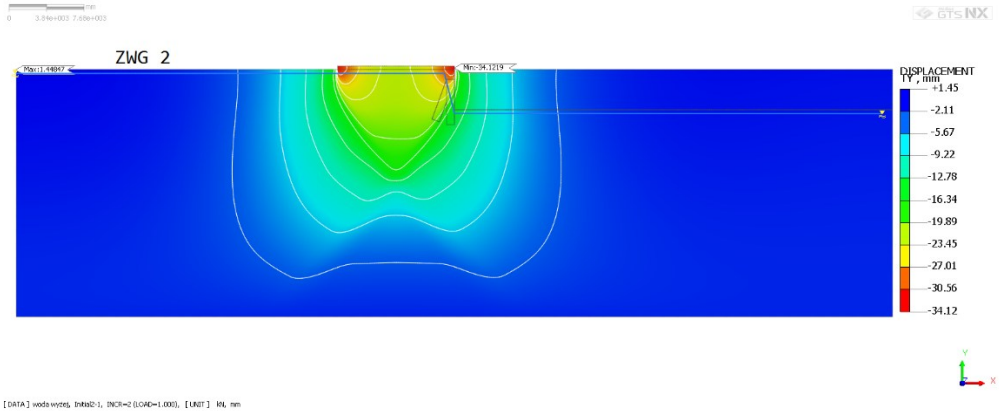

Fig. 30. Image of vertical displacements at the initial state and the upper level of the groundwater table for the values of total parameters

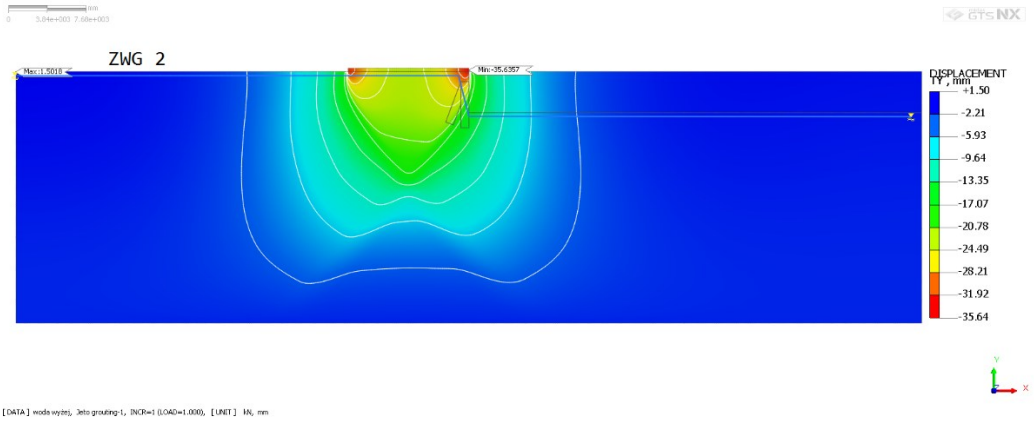

Fig. 31. Image of vertical displacements at the existing state and the upper level of the groundwater table after the completion of jet-grouting columns and without anchors for the values of total parameters

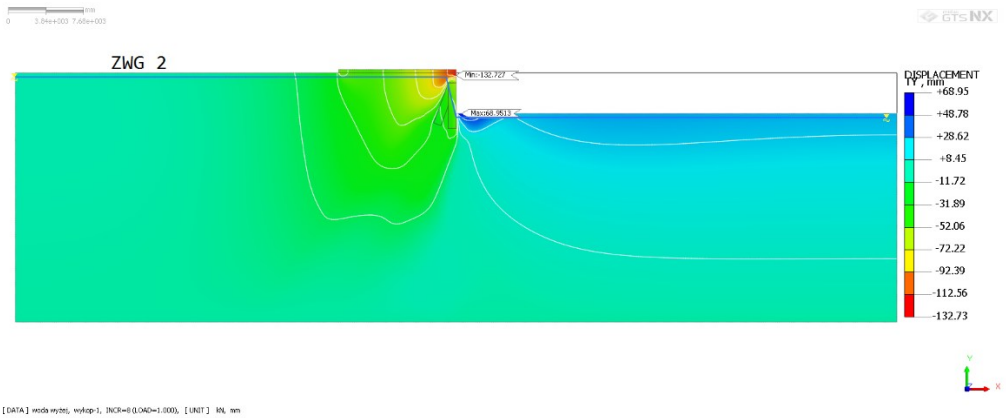

Fig. 32. Image of vertical displacements at the existing state and the upper level of the groundwater table after the completion of the tunnel excavation for the values of total parameters

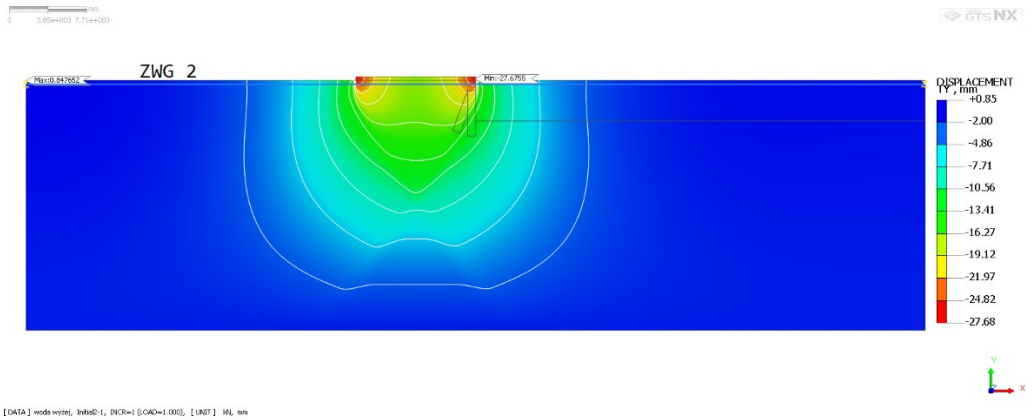

Fig. 33. Image of vertical displacements at the initial state and the upper level of the groundwater table for the values of effective parameters

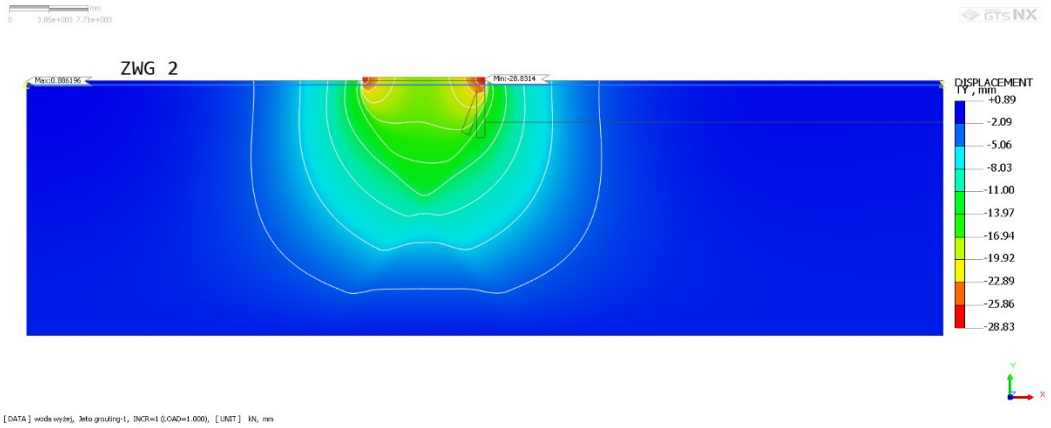

Fig. 34. Image of vertical displacements at the existing state and the upper level of the groundwater table after the completion of the jet-grouting columns and without anchors for the values of effective parameters

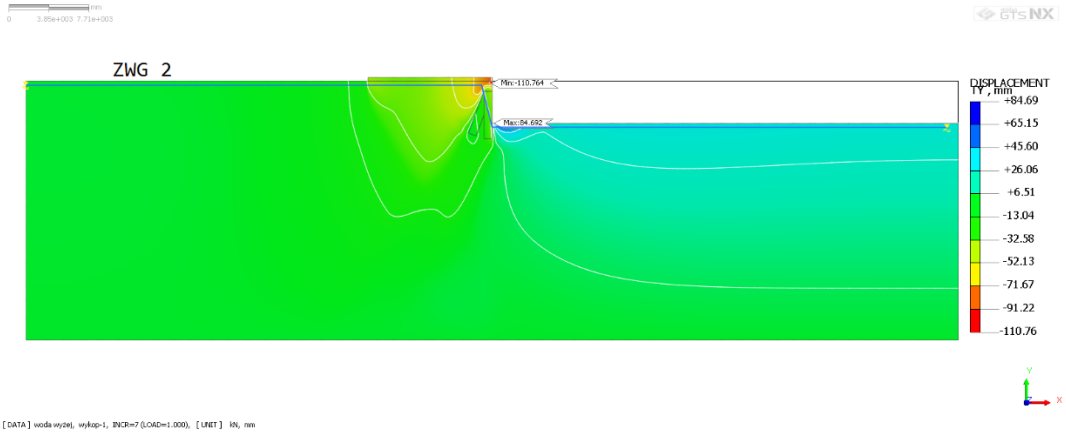

Fig. 35. Image of vertical displacements at the existing state and the upper level of the groundwater table after the completion of the tunnel excavation for the values of effective parameters

Then, similar calculation situations are analysed taking into account the effective parameters of the subsoil. Analogous FEM meshes were used. Figure 33 presents the image of vertical displacements at the initial state and the highest groundwater table. Figure 34 shows the image of vertical displacements at the existing state after the construction of jet-grouting columns and without anchors. Figure 35 presents the image of vertical displacements at the existing state and the highest groundwater table after the tunnel excavation. The results from Figures 33-35 are also included in the comparison prepared for the above-mentioned calculation states in Table 4.

Tab. 4. Vertical displacements of the slab corner in the actual state, taking into account the high water level

Parameters	**Vertical displacements [mm]**			
	after consolidation	**with jet-grouting columns**	**with tunnel excavation**	**Final**
total	34,1	35,6	132,7	97,1
effective	27,7	28,8	110,8	82,0

5. Conclusion

Based on the available literature, analysis of the provided materials, findings from the on-site inspection, and the authors' expertise, the following observations can be made:

An evaluation of the solutions presented in Chapter 3, as detailed in Tables 1 and 2, indicates that the design accounted for both low and high groundwater levels. Calculations were performed using both total and effective soil parameters, assuming the jet-grouting column curtain was watertight and the ground anchors functioned correctly. Under these assumptions, the final vertical settlement of the foundation slab did not exceed 25.1 mm. According to Eurocode 7 (Annex H) and the relevant national annex [3-7], this value remains within the permissible settlement limits.

Conversely, the analysis of the results shown in Chapter 4, and detailed in Tables 3 and 4, reveals that for high groundwater conditions—regardless of whether total or effective subsoil parameters were used—the settlement values for the existing underpinning solution of the newly constructed station wing significantly exceeded the allowable limits set by Eurocode 7.

These findings suggest that the implemented solution may have contributed to the observed damage in the new railway station wing. This damage is evident in the form of visible surface cracks and potentially hidden structural defects, likely caused by substantial and uneven settlement of the foundation slab. The primary cause appears to be the improper execution of the underpinning works using jet-grouting columns, which did not align with the designer's specifications.

References

1. Gryczmański M., Wprowadzenie do opisu sprężysto-plastycznych modeli gruntu. IPPT PAN Warszawa 1995.
2. Godlewski T., Kacprzak G., Witowski M., Praktyczna ocena parametrów geotechnicznych podłoża do projektowania ścian szczelinowych posadowionych w iłach „plioceńskich" Warszawy. Budownictwo i Inżynieria Środowiska. 4/2013, s. 13-19).
3. Polska Norma PN-EN 1997-1:2008. Eurokod 7: Projektowanie geotechniczne - Część 1: Zasady ogólne.
4. Polska Norma PN-EN 1997-2:2009. Eurokod 7: Projektowanie geotechniczne - Część 2: Rozpoznanie i badanie podłoża gruntowego.
5. Polska Norma PN-83/B-02482 "Fundamenty budowlane. Nośność pali i fundamentów palowych.
6. Polska Norma PN-B-04452: 2002. Geotechnika. Badania polowe.
7. Rozporządzenie Ministra Transportu, Budownictwa i Gospodarki Morskiej z dnia 25 kwietnia 2012 r. ws. ustalania geotechnicznych warunków posadawiania obiektów budowlanych
8. Rozporządzenie Ministra Środowiska z dnia 18 listopada 2016 r. ws. dokumentacji hydrogeologicznej i dokumentacji geologiczno-inzynierskiej
9. Ustawa z dnia 7 lipca 1994 r. - Prawo budowlane (Dz.U. z 2020 r. poz. 293, z późn. zm.)
10. Wiłun Z., Zarys geotechniki, WKiŁ, Warszawa 2007.
11. Urbański A. (red.), Podstawy projektowania geotechnicznego. Wprowadzenie do nowych technologii w geotechnice. Wydawnictwo Politechniki Krakowskiej. Kraków 2016.
12. Dąbska A., Pisarczyk S., Popielski P., Nasypy budowlane. Oficyna Wydawnicza Politechniki Warszawskiej. OWPW Warszawa 2022.
13. Pisarczyk S., Geoinżynieria. Metody modyfikacji podłoża gruntowego. Oficyna Wydawnicza Politechniki Warszawskiej. OWPW Warszawa 2020.
14. Tomlinson M.J., Pile design and construction practice, Chapman & Hall, London 1994.